Predictions on Heat Transport and Plasma Rotation from Global Gyrokinetic Simulations

Y Sarazin[1], V Grandgirard[1], J Abiteboul[1], S Allfrey[1], X Garbet[1], Ph Ghendrih[1], G Latu[1], A Strugarek[1], G Dif-Pradalier[2], P H Diamond[2], S. Ku[3], C S Chang[3], B F McMillan[4], T M Tran[4], L Villard[4], S Jolliet[5], A Bottino[6], P Angelino[7]

1) CEA, IRFM, F-13108 Saint Paul-lez-Durance cedex, France.
2) Center for Astrophysics and Space Sciences, UCSD, La Jolla, California 92093, USA.
3) Courant Institute of Mathematical Sciences, New York Univ., New York 10012, USA.
4) Centre de Recherches en Physique des Plasmas, Association Euratom-Confédération Suisse, Ecole Polytechnique Fédérale de Lausanne, 1015 Lausanne, Switzerland.
5) Japan Atomic Energy Agency, Higashi-Ueno 6-9-3, Tokyo 110-0015, Japan
6) Max-Planck Institut für Plasmaphysik, Association Euratom, Garching, Germany.
7) Laboratory of Computational Systems Biotechnology, EPFL, 1015 Lausanne, Switzerland.

E-mail contact of main author: yanick.sarazin@cea.fr

Abstract.

Flux-driven global gyrokinetic codes are now mature enough to make predictions in terms of turbulence and transport in tokamak plasmas. The recent breakthroughs of three such codes, namely GYSELA, ORB5 and XGC1, are reviewed. Turbulent transport is mediated by avalanche-like events, for a broad range of $\rho_* = \rho_i/a$ values, ratio of the gyro-radius over the minor radius. Still, the radial correlation length scales with ρ_i, leading to the gyroBohm scaling of the effective transport coefficient below $\rho_* \approx 1/300$. The experimental power law decay of the energy confinement time with additional power is recovered. For flat density profiles, the poloidal rotation of turbulence eddies is governed by the electric drift. At low collisionality, the shear of the total poloidal rotation departs from the neoclassical prediction, as a result of the radial corrugation of the zonal flows. The latter limits the excursion of the avalanches. Finally, the numerical verification of toroidal momentum balance allows one to analyze in detail the transport and source/sink terms of momentum in the absence of injected torque.

1. Introduction

Predicting the performance of fusion plasmas in terms of quality factor, ratio of the fusion power over the injected power, is among the key challenges in fusion plasma physics. In this perspective, turbulence and heat transport need being modeled within the most accurate theoretical framework, using state-of-the-art non-linear simulation tools. The gyrokinetic equation for each species, coupled to Maxwell's equations, constitutes the proper self-consistent description of this problem. As far as the modeling part is concerned, one of the key issues deals with the type of forcing applied to the system. In order to get closer to experimental conditions, new types of codes have recently emerged, in which turbulence is driven by some prescribed external heat source [1].

The most recent results obtained with three such codes are reviewed, focussing on predictions on turbulent transport and plasma rotation in tokamaks. Section 2 details the models, with special emphasis on the main differences from one code to another, in particular regarding the source term. The turbulent transport dynamics is highlighted in section 3, as well as its scaling law with the normalized gyro-radius ρ_* and the addi-

tional power. Attempts to trigger transport barriers are also reported. Finally, plasma rotation issues, both in the poloidal and toroidal directions, are the backbone of section 4.

2. Main characteristics of the three gyrokinetic codes

The non-linear results of three gyrokinetic codes are analyzed and compared hereafter, namely GYSELA [2], ORB5 [3] and XGC1 [4]. Although they use different numerical schemes, all three share similar characteristics, which reveal essential to capture the rich dynamics of flux-driven turbulent transport. Firstly, they are global: a large fraction of the plasma radius is considered. This opposes to flux-tube codes which focus on the small volume around magnetic field lines by proceeding from a scale separation assumption, the fluctuation scale length being smaller than the equilibrium one. In such codes, periodicity is assumed along the radial direction. Conversely, global codes face the delicate problem of radial boundary conditions. Basically, non-axisymmetric fluctuations of the electric potential and of the distribution function – i.e. $(m,n) \neq (0,0)$ modes, with m and n the poloidal and toroidal wave numbers – are forced to zero at both radial boundaries of the simulated domain, except for ORB5 which solves up to the magnetic axis. As far as the axisymmetric component is concerned, the value of the potential is prescribed at the outer boundary, while the radial electric field is set to zero at the inner boundary (except for ORB5). Secondly and very importantly, these codes are full-f[1], such that the back reaction of turbulent transport is accounted for in the time evolution of the equilibrium. In such cases, the turbulence regime is evanescent if no free energy is injected in the system. A heat source is mandatory in view of exploring the long time – on energy confinement times – behavior of turbulence and transport.

The simulations focus on the electrostatic Ion Temperature Gradient (ITG) driven turbulence with adiabatic electrons. The set of solved equations is derived from the modern formulation of gyro-kinetic theory [6]. We detail the formulation adopted in the GYSELA code, and outline the main differences with respect to the two other codes, ORB5 and XGC1. They read, for the entire ion distribution function $f(r,\theta,\varphi,v_{G\|},\mu,t)$:

$$B^*_\| \partial_t f + \boldsymbol{\nabla}\cdot\left(B^*_\| \,\dot{\mathbf{x}}_G\, f\right) + \partial_{v_{G\|}}\left(B^*_\| \,\dot{v}_{G\|}\, f\right) = \mathcal{C}(f) + S \tag{1}$$

$$B^*_\| \,\dot{\mathbf{x}}_G = v_{G\|}\mathbf{B}^* + \mathbf{b}\times\boldsymbol{\nabla}\Xi/e \quad ; \quad B^*_\| \,\dot{v}_{G\|} = -\mathbf{B}^*\cdot\boldsymbol{\nabla}\Xi/m_i \tag{2}$$

with $\boldsymbol{\nabla}\Xi = \mu\boldsymbol{\nabla}B + e\boldsymbol{\nabla}\bar{\phi}$ and $\mathbf{B}^* = \mathbf{B} + (m_i/e)\, v_{G\|}\boldsymbol{\nabla}\times\mathbf{b}$. The collision operator $\mathcal{C}(f)$ and the source term S are detailed below. $\bar{\phi}$ is the gyro-averaged electric potential. The scalar $B^*_\|$ is $B^*_\| = \mathbf{B}^*\cdot\mathbf{b}$, with $\mathbf{b} = \mathbf{B}/B$. Electrons are assumed adiabatic, so that particle transport vanishes. The system is closed by quasi-neutrality:

$$\left(\phi - \langle\phi\rangle\right) e/T_{e,eq} - \boldsymbol{\nabla}_\perp.\left\{\left(m_i n_{eq}/eB^2\right)\boldsymbol{\nabla}_\perp\phi\right\}/n_{eq} = \left(n_G - n_{G,eq}\right)/n_{eq} \tag{3}$$

with $\vec{\nabla}_\perp = (\partial_r, \frac{1}{r}\partial_\theta)$ and $\nabla_\| = \frac{1}{R}(\partial_\varphi + \frac{1}{q}\partial_\theta)$. The polarisation density (second term on the left hand side of Eq. 3) is an approximation: such an expression is valid in the limit of long wavelengths only, characterized by $k_\perp\rho_i \ll 1$. The guiding-center density is defined by: $n_G = \iint \mathcal{J}_v \,\mathrm{d}\mu\,\mathrm{d}v_{G\|}(J.f)$, with J the gyro-average operator and $\mathcal{J}_v = 2\pi B^*_\|/m_i$ the Jacobian in the velocity space. f is replaced by the equilibrium component f_{eq} when

[1] Although ORB5 uses a splitting $f = \delta f + f_0$ to improve numerical performance, the correct full-f equations are implemented, without any assumption on the relative size of f_0 and δf [5].

computing n_{eq}. $\langle\phi\rangle$ stands for the flux surface average of the electric potential, defined by $\langle\phi\rangle = \iint \mathcal{J}_x\ \phi\ \mathrm{d}\theta\,\mathrm{d}\varphi / \iint \mathcal{J}_x\,\mathrm{d}\theta\,\mathrm{d}\varphi$, with $\mathcal{J}_x = (\mathbf{B}\cdot\boldsymbol{\nabla}\theta)^{-1}$ the configuration space Jacobian.

Both ORB5 and XGC1 are Particle In Cell (PIC) codes, while GYSELA uses the semi-Lagrangian scheme [7]. They have been successfully benchmarked against several linear predictions, namely growth rates and real frequencies of the most unstable modes in the unstable ITG regime, and the oscillatory decay towards residual poloidal flow in the collisionless regime, according to Rosenbluth-Hinton prediction [8]. In XGC1 and ORB5, Coulomb collisions are modeled by a linearized Monte Carlo scheme [9], while a simplified Fokker-Planck operator is used in GYSELA, acting on $v_{G\parallel}$ only [10, 11]. Both of them conserve particle, momentum and energy, and the full distribution function relaxes towards the isotropic Maxwellian, according to the H-theorem (Boltzmann). Also, they have been shown to reproduce neoclassical physics. While GYSELA employs a simplified magnetic equilibrium with circular and concentric magnetic flux surfaces, both ORB5 and XGC1 are capable of treating more realistic geometries. Especially, XGC1 accounts for an X-point at the plasma periphery.

The source term aims at sustaining the equilibrium profiles, which would otherwise relax towards the marginal state. Different expressions have been retained in the three codes. In GYSELA, the source consists of the sum of the product of Hermite and Laguerre polynomials in $v_{G\parallel}$ and μ, respectively. It is versatile enough to allow for separate injection of heat, parallel momentum and vorticity. Present simulations use an anisotropic heat source. Up to small terms proportional to the parallel current, it reads as follows:

$$S_{GYSELA} \simeq S_r\ \left[\left(v_{G\parallel}/v_{Ts}\right)^2 - 1\right]\ \exp\left\{-\left(m_i {v_{G\parallel}}^2/2 + \mu B_0\right)/T_s\right\} \tag{4}$$

with v_{Ts} an arbitrary normalizing velocity. The prescribed radial profile S_r is the sum of two hyperbolic tangents, and is localized close to the inner boundary of the simulation domain [15]. Redistribution of the energy towards the transverse velocity space takes place on collisional time scales, the kernel of the collision operator being an isotropic Maxwellian. The source term applies to the time evolution of δf in ORB5. It is given the form of the following Krook operator [12]:

$$S_{ORB5} = -\gamma_H \left(\delta f - f_{eq} \int \mathrm{d}^3\mathbf{v}\,\delta f\ /\ \int \mathrm{d}^3\mathbf{v}\, f_{eq}\right) \tag{5}$$

Such a time dependent heat source damps the components of the perturbed distribution δf on a time scale γ_H^{-1}, while only leading to a mild reduction of zonal flows in the collisionless linear regime. This results in a limited relaxation of the equilibrium gradient. Finally, heating is achieved in XGC1 by increasing the particle energy close to the inner radial boundary at uniform rate, while keeping the particle pitch angle fixed [4]. An artificially large collisionality is prescribed in this region only so that the system smoothly transfers this forcing to the turbulent region.

There are two main advantages of dealing with a prescribed heat source: (*i*) the forcing of turbulence mimics the one at work in the experiments, contrary to simulations where the gradient remains fixed, and (*ii*) the sum of turbulent and neoclassical heat fluxes is forced to equal, on average and on the energy confinement time scale, the prescribed driving flux. In this case, the degree of freedom is the temperature gradient, which ultimately

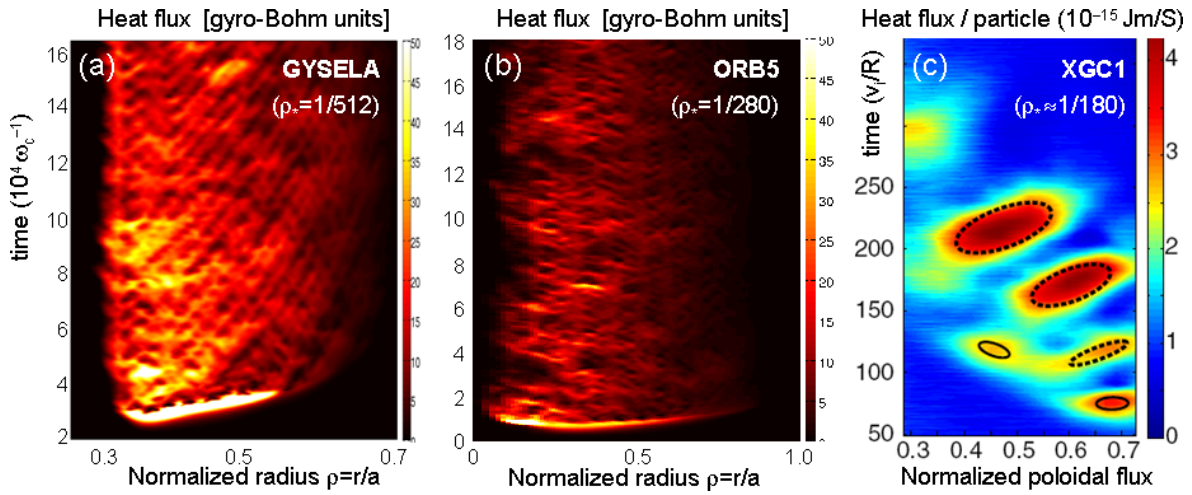

Figure 1: Color plots of the turbulent heat flux in the two-dimensional space (r,t) for the three global gyrokinetic codes GYSELA (a), ORB5 (b) and XGC1 (c).

governs the internal energy and therefore the performance of the discharge.

3. Transport dynamics and scaling properties

A general feature of flux-driven turbulence simulations, already well documented in fluid simulations [13, 14], is that the turbulent transport exhibits avalanche-like events, characterized by large scale intermittent outbursts. These bursts, which are easily identified on flux surface averaged maps of the heat flux (cf. Fig.1), propagate almost ballistically on large radial scales, much larger than the Eulerian correlation length of turbulence. Their propagation velocity is a fraction of the diamagnetic velocity $v_i^* \approx \rho_* v_T$, with $\rho_* = \rho_i/a$ the gyroradius normalised to the minor radius a, and v_T the ion thermal velocity. Notice that, when turbulence is primarily excited in the edge plasma region, like in XGC1 simulations with an initially large temperature gradient close to the last closed flux surface [9], a front of temperature then propagate inwards, at the same speed. Such a dynamics is associated to local profile relaxations, such as the "domino effect". For intermediate ρ_* values at least ($\rho_* = 1/64$), it is found to correlate with streamer-like structures of the convection cells, albeit their Fourier spectrum departs significantly from that of the most unstable linear modes [15]. For sufficiently small ρ_* simulations (typically $\rho_* < 1/256$), the shearing regions generated by the self-generated zonal flows appear to control the radial extent of the avalanches – although the opposite cannot be excluded *a priori*, namely that the avalanche mean size governs the position of zonal flows [16]. Besides, the direction of propagation of the avalanches depends on the sign of the local shearing rate [17, 18]. Such ingredients reveal extremely powerful when deriving reduced transport models which capture the essence of avalanche-like transport [17, 16]. One important feature of the zonal flow radial structure is that they exhibit a characteristic wave-like shape, as evident on Fig.2a. As already noticed, such a shape is reminiscent of the anti-viscosity nature of the Reynolds stress tensor [19]. Also, consistently with the

"staircase" picture [16], their characteristic radial size scales with the gyroradius ρ_i, independently of the system size. Predicting such a typical wavelength would be extremely valuable in the course of predicting turbulent transport level.

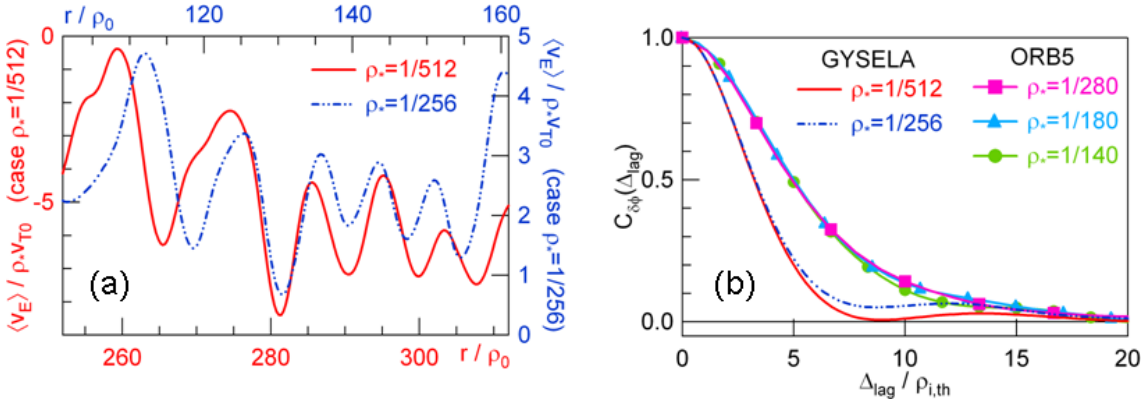

Figure 2: (a) Radial profile of the flux surface averaged poloidal component of the $E \times B$ drift for two values of ρ_* (GYSELA runs). The small scale structure, namely the zonal flows, exhibit radial patterns independent of the system size. (b) Auto-correlation function of the electric potential fluctuations for different ρ_* values.

The scaling properties, especially with respect to ρ_*, of the avalanche-dominated turbulent transport is a matter of concern for predicting the performances of next step devices, including ITER. First because ρ_* strongly impacts the energy confinement time, $\omega_c \tau_E \sim \rho*^{-2.8}$ according to ITER scaling law. Second because avalanches could break the gyro-Bohm scaling of turbulence, possibly due to their large radial excursion over a significant portion of the system size. Scanning ρ_* from 1/70 to 1/560 with ORB5 reveals that the effective diffusion coefficient undergoes a transition towards the gyro-Bohm scaling around $\rho_* \approx 1/300$, with an asymptotic value of the order of $\chi/\chi_{gB} \approx 2.8 - 2.9$ [20]. The same results are obtained with the global version of the Eulerian GENE code [21], while the local version prediction looks consistent with the smallest ρ_* simulations. Following another perspective, the typical size of the avalanches as well as the distance between strongly sheared zonal flow layers is found to plateau below typically $\rho_* \lesssim 1/256$ [16]. Consistently, the correlation length of the electric potential fluctuations exhibits a convincing scaling with ρ_i, independent of the system size, as evident on Fig.2b. Flux driven simulations also allow for investigating the impact of heating power on energy confinement time. Such an analysis is time consuming, and requires all the more CPU time since ρ_* is small. For this reason, it was performed at relatively large ρ_* only ($\rho_* = 1/64$). The degradation of the confinement was observed when increasing the injected heating power P_{add}, with the scaling exponent $\tau_E \sim P_{add}^{-0.76 \pm 0.04}$ of the same order of magnitude as the one reported in the ITER database in L-mode plasmas.

Last but not least, the possibility to trigger transport barriers has been explored. Experimentally, internal transport barriers (ITBs) often develop in the vicinity of low order rational resonant surfaces and weak magnetic shear regions, at least in JET and ASDEX-Upgrade [22]. In this context, GYSELA simulations with hollow and monotonous

q profiles have been compared. The hollow-q case exhibits a large radial gap region without any resonant mode across q_{min}. No transport barrier was observed, although different heat source magnitudes and increasing gap widths have been explored [23]. Conversely, turbulent transport dramatically drops (by 2 orders of magnitude) in the gap region when an artificial conical Fourier filter is applied, which only retains those modes which are resonant in the simulation domain. Such gyrokinetic simulations tend to reconcile – and extend to the turbulence flux-driven regime – previously published contradictory results on the topic. However, understanding and reproducing the experimental triggering of internal transport barriers still remain an open issue.

4. Poloidal and toroidal flows

Poloidal rotation is a key player in the dynamics of turbulence eddies [24]. On the one hand, because of the large friction due to trapped particles, it is usually assumed to be governed by the neoclassical theory in tokamak plasmas, i.e. proportional to the equilibrium ion temperature gradient. On the other hand, collisions linearly damp the turbulence self-generated zonal flows. A twofold scan in the turbulence drive and in collisionality with GYSELA has revealed that turbulence itself can indeed generate a significant amount of poloidal momentum. Although its magnitude remains weak with respect to the neoclassical prediction – at least in the absence of any transport barrier – such a turbulence drive increases significantly the velocity shear, mainly through the turbulent corrugation of the mean profiles. This property tends to increase at smaller collisionality, and may therefore reveal important when considering ITER relevant parameters [11].

It is interesting to notice that turbulent eddies do not actually rotate at the same speed as the ions. Indeed, the linear expectation indicates that the real frequency of the fluctuations should be $\omega \approx \omega_E + \omega_n^*$, with $\omega_n^* = (k_\theta \rho_i) v_T \partial_r (\log n)$ the density part of the diamagnetic frequency and $\omega_E = (k_\theta \rho_i) v_T \partial_r \langle \phi \rangle$ the Doppler shift governed by the radial gradient of the mean electric field. The latter is usually dominant, unless steep density gradients develop. This is consistent with the fact that the radial electric shear only, and not the shear of the total poloidal plasma flow, plays the critical role in the stabilization of turbulence. A more detailed analysis reveals that this poloidal flow does not critically depend on the mode number, at least up to $k_\theta \rho_i = 1$. Experimental measurements suggest that, possibly depending on the underlying dominant instability (ITG or trapped electron modes), such a flow might actually vary with the mode number, at least for small scales [25]. Due to the simplified gyro-average operator used in GYSELA, sub-Larmor scales are presently over-damped, preventing us to explore the $k_\theta \rho_i > 1$ region.

Toroidal rotation is another important player, for it tends to stabilize deleterious MHD modes (so-called Resistive Wall Modes) and because its shear may reduce the turbulent transport level. However, the amount of injected torque is expected to be very small in ITER. Plasma rotation should then rely on non linear processes leading to angular momentum transport and redistribution. From Eq.1, an exact conservation equation can be derived for the local toroidal angular momentum $\mathcal{L}_\varphi = \sum_s m_s \int \mathrm{d}\tau^* \, u_\varphi f$, where the toroidal component of the velocity is $u_\varphi = (I/B) v_{G\parallel}$ (with $\mathbf{B} = I \boldsymbol{\nabla} \varphi + \boldsymbol{\nabla} \varphi \times \boldsymbol{\nabla} \chi$) and $\mathrm{d}\tau^*$ is the elementary reduced phase space volume, excluding the radial direction χ:

$$\partial_t \mathcal{L}_\varphi + \partial_\chi \left(\Pi_\varphi^\chi + \mathrm{T}_\varphi^\chi \right) = \mathsf{J} \tag{6}$$

We introduce the radial contravariant component of the velocity $v_G^\chi = \dot{\mathbf{x}}_G \cdot \boldsymbol{\nabla}\chi$. It contains both the $E \times B$ and the magnetic drifts, which govern the turbulent and neoclassical contributions, respectively. Then, the following definitions hold:

$$\Pi_\varphi^\chi = \sum_s m_s \int \mathrm{d}\tau^*\, u_\varphi v_G^\chi\, f\ ; \quad \mathrm{T}_\varphi^\chi = \sum_s e_s \int^\chi \mathrm{d}\chi \int \mathrm{d}\tau^*\, \partial_\varphi \bar{\phi}\, f\ ; \quad \mathsf{J} = \sum_s e_s \int \mathrm{d}\tau^*\, v_G^\chi\, f \quad (7)$$

Here, Π_φ^χ is the $(\varphi\chi)$ off-diagonal component of the Reynolds stress tensor and T_φ^χ that of the Maxwell stress tensor built with the polarization field [26]. It is reminiscent of the source of spin up proposed in [27]. The radial integral of $\mathcal{L}_\varphi$ vanishes, as it should, provided that the radial current J of gyrocenters is zero. This constraint is naturally fulfilled by the gyrokinetic equation due to charge conservation, $\partial_t \rho + \partial_\chi \mathsf{J} = 0$, or alternatively after radial integration: $\partial_t \sigma - \mathsf{J} = 0$ (up to a divergence free component of the current, typically a magnetization contribution), where σ is the flux surface integral of the contravariant radial component of the polarization vector ($\partial_\chi \sigma = -\rho$) [6]. It then readily appears that $\mathsf{J} = 0$ in the steady state regime. As evident on Fig.3, the local balance Eq.6 is well satisfied in the nonlinear regime. Also, it appears that the radial current is indeed vanishing, while the main contributors are the turbulent and neoclassical stresses. Such a balance will be especially scrutinized in the presence of possible transport barriers, as well as when adding a source of toroidal momentum into the system.

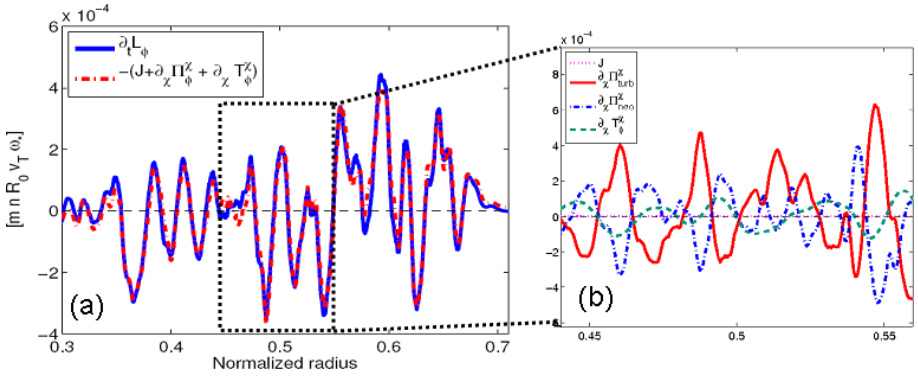

Figure 3: (a) Local balance of toroidal momentum. (b) Detail of various components.

5. Conclusions

This paper reports on global gyrokinetic simulations of ITG turbulence in the flux-driven regime with the three codes GYSELA, ORB5 and XGC1. Transport is largely dominated by avalanches, of characteristic radial velocity $\rho_* v_T$. Although they can propagate radially on much larger radial distances than the Eulerian correlation length of turbulent eddies, the effective heat diffusivity still exhibits a gyro-Bohm scaling, at least below $\rho_* \approx 1/300$. They are also found to degrade the confinement at increasing heating power, in quantitative agreement with experimental scalings. The poloidal rotation of turbulent eddies is consistent with linear predictions. As far as the plasma poloidal rotation is concerned, its shear significantly departs from the neoclassical prediction at low collisionality, as a result of the radial corrugation of the zonal flows. Finally, the intrinsic toroidal rotation appears mainly driven by the turbulent and neoclassical stresses.

Acknowledgements: It is our pleasure to acknowledge C. Passeron for her constant and invaluable help in the course of running GYSELA. The work with GYSELA was granted access to the HPC resources of CCRT and CINES under the allocation 2009052224 made by GENCI (Grand Equipement National de Calcul Intensif), as well as on HPC-FF in Jülich. ORB5 computations were performed on HPC-FF in Jülich. This work, supported by the European Communities under the contract of Association between EURATOM and CEA, was carried out within the framework of the European Fusion Development Agreement. The views and opinions expressed herein do not necessarily reflect those of the European Commission.

References

[1] Garbet X, Idomura Y, Villard L and Watanabe T H 2010 *Nucl. Fusion* **50**, 043002

[2] Grandgirard V, Sarazin Y *et al* 2007 *Plasma Phys. Control. Fusion* **49**, B173

[3] Jolliet S, Bottino A *et al* 2007 *Comp. Phys. Communications* **177**, 409

[4] Chang C S, Ku S 2008 *Phys. Plasmas* **15**, 062510; Chang C S *et al* 2009 *Phys. Plasmas* **16**, 056108

[5] Villard L, Bottino A *et al* 2010 *"Gyrokinetic simulations of turbulent transport: size scaling and chaotic behaviour"*, to appear in *Plasma Phys. Control. Fusion*

[6] Brizard A J and Hahm T S 2007 *Rev. Mod. Phys.* **79**, 421

[7] Grandgirard V, Brunetti M *et al* 2006 *J. Comput. Phys.* **217**, 395

[8] Rosenbluth M N and Hinton F L 1998 *Phys. Rev. Lett.* **80**, 724

[9] Ku S, Chang C S and Diamond P H 2009 *Nucl. Fusion* **49**, 115021

[10] Garbet X, Dif-Pradalier G *et al* 2009 *Phys. Plasmas* **16**, 062503

[11] Dif-Pradalier G, Grandgirard V *et al* 2009 *Phys. Rev. Lett.* **103**, 065002

[12] McMillan B F, Jolliet S *et al* 2008 *Phys. Plasmas* **15**, 052308

[13] Garbet X, Sarazin Y *et al* 1999 *Nucl. Fusion* **39**, 2063

[14] Beyer P, Benkadda S, Garbet X and Diamond P H 2000 *Phys. Rev. Lett.* **85**, 4892

[15] Sarazin Y, Grandgirard V *et al* 2010 *Nucl. Fusion* **50** 054004

[16] Dif-Pradalier G, Diamond P H *et al* 2010 *Phys. Rev. E* **82** 025401(R)

[17] McMillan B F, Jolliet S *et al* 2009 *Phys. Plasmas* **16** 022310

[18] Idomura Y, Urano H, Aiba N and Tokuda S 2009 *Nucl. Fusion* **49** 065029

[19] Diamond P H, Itoh S-I *et al* 2005 *Plasma Phys. Control. Fusion* **47** R35-R161

[20] McMillan B F *et al* 2010 *"System size effects on gyrokinetic turbulence"*, to appear in *Phys. Rev. Lett.*

[21] Lapillonne X 2010 Ph.D. thesis, EPFL; Görler T 2009 Ph.D. thesis, Univ. Ulm

[22] Challis C D *et al* 2002 *Plasma Phys. Control. Fusion* **44** 1031; Joffrin E, Challis C D *et al* 2003 *Nucl. Fusion* **43** 1167

[23] Sarazin Y, Strugarek A *et al* 2010, to appear in *J. Phys. Conf. Series*

[24] Biglari H, Diamond P H and Terry P 1990 *Phys. Fluids* B **2** 1

[25] Vermare L *et al*, this conference

[26] Abiteboul J, Garbet X *et al* 2010, proceedings of EPS conference (Dublin, 2010)

[27] McDevitt C J, Diamond P H *et al* 2009 *Phys. Rev. Lett.* **103** 205003